ELASTIC CONSTANTS AND VELOCITY SURFACES OF INDURATED ANISOTROPIC SHALES

JOEL E. JOHNSTON and NIKOLAS I. CHRISTENSEN
Purdue University, Dept. of Earth and Atmospheric Sciences, W. Lafayette, IN 47907, U.S.A.

(Received 27 August, 1993)

Abstract. The velocities of two Devonian-Mississippian shales have been measured to confining pressures of 200 MPa in a laboratory study of anisotropy and wave propagation. Both samples were found to be transversely isotropic at elevated pressures with the main symmetry axis perpendicular to bedding. The elastic constants of the shales were used to calculate phase and group velocity surfaces as a function of angle to the bedding normal. Multiple velocity measurements in non-symmetry directions, not undertaken in previously published studies of shales, have been used to confirm features observed on calculated velocity surfaces. It is demonstrated that velocities measured in non-symmetry directions are phase velocities. Group velocities were found to be significantly lower than the corresponding phase velocities of the shales due to their high anisotropies. Shear wave splitting was found to be negligible for propagation directions within approximately 30° of the bedding normals.

Key words: Vp, vs, laboratory, anisotropy, shales, elastic constants, velocity surfaces

1. Introduction

Recent studies, including shear and compressional reflection profiling, refraction profiling, and seismic tomography, have found that velocity anisotropy is an important crustal property (e.g., Banik, 1984; Crampin, 1985; Justice, 1986; Winterstein, 1986, 1990; Thomsen, 1986, 1988; Carrion *et al.*, 1992). Pervasive velocity anisotropy in the upper crust due to both mineral alignment and aligned vertical cracks has been documented in many field experiments (e.g., White *et al.*, 1983; McCormack *et al.*, 1984; Lynn and Thomsen, 1990; Brocher and Christensen, 1990) emphasizing the need for further investigations of anisotropy. Laboratory studies under controlled conditions can provide important information regarding the origin, symmetry, and magnitude of anisotropy vital to the interpretation of the field data. In this study, the ultrasonic velocities of two highly anisotropic shales were measured to pressures of 200 MPa and used to calculate elastic constants, phase velocity surfaces, and group velocity surfaces of the samples. Multiple velocity measurements in non-symmetry directions, not undertaken in previous studies of shales, have allowed verification of calculated phase and group velocity surfaces.

2. Previous Studies

Seismic wave propagation in anisotropic rock forming minerals has been studied for many years (e.g., Verma, 1960; Alexandrov and Ryzhova, 1961; Kumazawa,

1969; Weidner *et al.*, 1975; Pacalo *et al.*, 1992). Studies of wave propagation have also been undertaken in anisotropic crystalline rocks such as dunites, peridotites, anorthosites, and bronzitites (e.g., Christensen, 1966; Babuska, 1972; Baker and Carter, 1972; Christensen and Ramananantoandro, 1971; Crosson and Lin, 1971; Christensen, 1984; Seront *et al.*, 1993). Because of interest in upper mantle anisotropy (Hess, 1964), most of these laboratory studies have involved olivine and or pyroxene rich rocks possessing hexagonal or orthorhombic symmetry.

Laboratory studies of anisotropy and wave propagation in fine grained rocks are uncommon since mineral orientation information in these rocks can only be obtained by X-ray techniques. Jones and Wang (1981) measured the velocities of two Cretaceous shales from the Williston basin. They found that the samples behaved as transversely isotropic solids with the main symmetry axis perpendicular to bedding. Lo *et al.* (1986) calculated the elastic constants of several rocks, including a Chicopee shale sample. Sano *et al.* (1992) measured ultrasonic velocities of several granites which possessed orthogonal symmetry caused by orthogonal sets of microfractures. Phase velocity surfaces were calculated using the elastic constants of the samples which showed fairly good agreement with velocities measured at various angles to the symmetry axes (Sano *et al.*, 1992). Vernik and Nur (1992) measured the velocities of a suite of kerogen rich shales, calculating elastic constants and phase velocity surfaces. They found the samples to be transversely isotropic with the main symmetry axis perpendicular to bedding.

3. Experimental Technique

The two shale samples examined in this study were taken from the Millboro member of the Devonian-Mississippian Chattanooga formation, exposed in the Thorn Hill sedimentary section of eastern Tennessee (Walker, 1985). Both samples are well indurated and fresh, with porosities of 1.0% or less (Johnston and Christensen, 1992). The shales are fairly homogenous in composition and display very fine lamination due to clay minerals aligned parallel to bedding, qualities which make them ideal for a laboratory-scale study of anisotropy and wave propagation.

In the laboratory multiple 2.54 cm diameter cores were taken parallel and perpendicular to bedding from each rock. Cores were also taken at 45° to bedding and at a range of other angles, when possible. The cores were then trimmed and polished into right circular cylinders between 2.0–4.0 cm long with ends flat and parallel to within 0.005 cm. The lengths, diameters, and weights of the cores were measured before jacketing the cores with copper to isolate them from pressure fluid. Velocities were then measured to hydrostatic confining pressures of 200 MPa using the pulse transmission technique (Birch, 1960) and shear and compressional wave transducers of 1.0 MHz resonant frequency as sources and receivers. Velocities measured using this method are believed to be accurate to

within 1.0% (Christensen, 1985). Velocities were measured under dry conditions primarily because of the low sample porosities.

Velocities of the shales as a function of confining pressure are given in Table I for selected propagation directions. At elevated pressures, both samples are transversely isotropic with the main symmetry axis perpendicular to bedding. Extreme anisotropy in both compressional and shear wave velocities is present and can be attributed to clay mineral alignment parallel to bedding. For both samples, the five independent elastic constants characteristic of a transversely isotropic solid are presented in Table I. These were calculated using the velocity-stiffness relations given in Musgrave (1970).

4. Phase Velocity Surfaces

The calculation of phase velocity surfaces (Musgrave, 1970) as a function of angle to the bedding normal for both shales is useful for visualizing three-dimensional wave propagation. Three velocity surfaces are found in rocks exhibiting transverse isotropy caused by mineral alignment parallel to bedding: a quasi-compressional wave surface (*Vp*), a quasi-shear wave surface for shear waves vibrating in the plane perpendicular to bedding (*Vsv*), and a surface for shear waves vibrating parallel to bedding (*Vsh*). Note that for propagation directions parallel and perpendicular to bedding all waves are "pure" modes. The equations for these surfaces, taken from Auld (1990), are as follows:

$$Vp = \sqrt{\frac{c_{11}\sin^2\theta + C_{33}\cos^2\theta + C_{44} + \sqrt{[(C_{11} - C_{44})\sin^2\theta + (C_{44} - C_{33})\cos^2\theta]^2 + (C_{13} + C_{44})^2\sin^2 2\theta}}{2\rho}}$$

$$Vsv = \sqrt{\frac{c_{11}\sin^2\theta + C_{33}\cos^2\theta + C_{44} - \sqrt{[(C_{11} - C_{44})\sin^2\theta + (C_{44} - C_{33})\cos^2\theta]^2 + (C_{13} + C_{44})^2\sin^2 2\theta}}{2\rho}}$$

$$Vsh = \sqrt{\frac{\frac{1}{2}(C_{11} - C_{12})\sin^2\theta + C_{44}\cos^2\theta}{\rho}}$$

In these formulas, θ is the angle between bedding normal and wavefront normal and ρ is sample density in g/cm^3. The calculated velocity surfaces are dependent upon the shear and compressional velocities measured parallel and perpendicular to bedding, and also upon the compressional wave velocity measured at 45°, which is used to determine the C_{13} constant. Calculation of these curves is straightforward, with the only difficulty being the measurement of a representative 45° compressional wave phase velocity as the C_{13} constant, and hence the *Vp* and *Vsv* phase velocity surfaces, are sensitive to this value.

Using the equations presented above, shear and compressional velocity surfaces for TH-26 and TH-51 at 100 MPa confining pressure were calculated and are shown in Figures 1 and 2. Velocities measured along the axes of symmetry of the samples, at 45° to bedding, and at other angles to bedding are also

TABLE I

Velocities (in km/S) and elastic constants of shales as a function of confining pressure. '*Vsh*' indicates a shear wave vibrating parallel to bedding, '*Vsv*' a shear wave vibrating in the plane perpendicular to bedding.

TH-26 ($\rho = 2.341$ g/cm^3)

	Normal to bedding		45 Degrees			Parallel to bedding			Elastic Constants (GPa)				
Pressure (MPa)	Vp	Vs	Vp	Vsh	Vsv	Vp	Vsh	Vsv	C11	C12	C13	C33	C44
50	3.132	1.833	3.790	2.355	2.131	4.549	2.816	1.794	48.43	11.31	12.47	22.96	7.70
100	3.286	1.886	3.912	2.396	2.189	4.666	2.864	1.844	50.96	12.55	13.77	25.28	8.14
150	3.400	1.927	4.001	2.424	2.232	4.759	2.898	1.880	53.02	13.70	14.54	27.06	8.48
200	3.496	1.965	4.077	2.446	2.260	4.839	2.925	1.908	54.82	14.76	15.21	28.61	8.78

TH-51 ($\rho = 2.384$ g/cm^3)

	Normal to bedding		45 Degrees			Parallel to bedding			Elastic Constants (GPa)				
Pressure (MPa)	Vp	Vs	Vp	Vsh	Vsv	Vp	Vsh	Vsv	C11	C12	C13	C33	C44
50	3.225	1.921	3.973	2.557	2.310	4.891	2.968	1.857	57.03	15.03	11.69	24.80	8.51
100	3.349	1.964	4.056	2.586	2.363	4.965	3.004	1.891	58.76	15.73	12.68	26.74	8.86
150	3.432	1.992	4.119	2.620	2.394	5.014	3.024	1.910	59.93	16.33	13.73	28.08	9.07
200	3.489	2.012	4.171	2.641	2.417	5.053	3.039	1.921	60.86	16.82	14.77	29.02	9.22

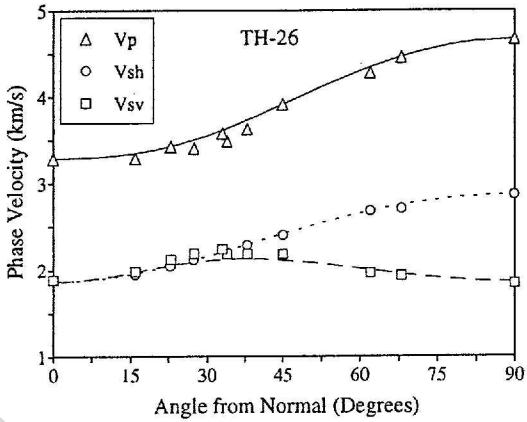

Fig. 1. Calculated (lines) and observed (symbols) phase velocities as a function of angle to bedding normal for TH-26. Average differences between observed and calculated *Vp*, *Vsv*, and *Vsh* velocities are 1.8%, 2.9%, and 0.8%, respectively.

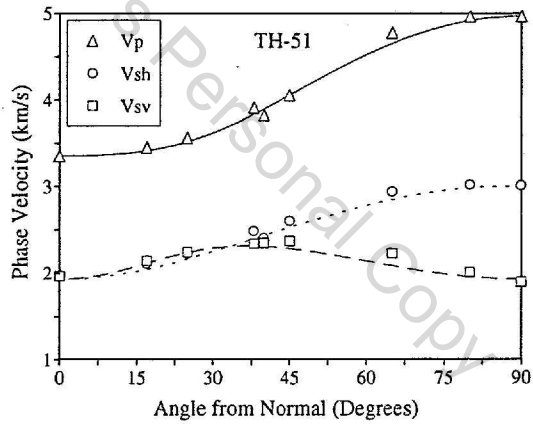

Fig. 2. Calculated and observed phase velocities for TH-51. Average differences between observed and calculated *Vp*, *Vsv*, and *Vsh* velocities are 1.7%, 2.4%, and 2.5%, respectively.

displayed. Unequal angular coverage of measured velocities is due to breakage of cores during preparation and limited sample sizes. The independently measured velocities agree well with the calculated velocity surfaces for both shales. For TH-26 (Figure 1) the match between the calculated *Vsh* and measured *Vsh* velocities is excellent, with an average difference (relative to measured velocity) of 0.8%. Slightly larger differences exist between the calculated and observed velocities for the *Vp* and *Vsv* surfaces, but overall agreement is good. For shale TH-51 (Figure 2), good agreement is seen between observed and calculated *Vp* and *Vsv* surfaces. The calculated *Vsh* surface consistently slightly underestimates the observed velocities, but follows the same overall trend.

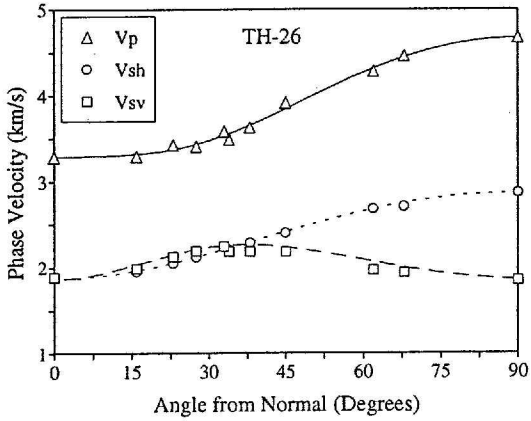

Fig. 3. Calculated and observed phase velocities for TH-26 using new C_{13} constant (see text). Average differences between observed and calculated *Vp* and *Vsv* velocities are 1.0% and 2.4%.

Variations between the observed and calculated surfaces for TH-26 and TH-51 can be attributed to slight compositional variations from core to core, and also to the phase velocity assumption (discussed below). Compositional variation can usually be identified by sample density, which can be used as a rough indicator of whether a given core is representative of the rock as a whole. Small pyrite nodules are found in these shales which have a large effect on density, but little effect on velocity. Thus, density is only a rough constraint. However, the standard deviations of the densities given in Table I for TH-26 and TH-51 are 0.029 g/cm^3 and 0.057 g/cm^3, respectively, indicating that both of these rocks are very homogenous. Figure 1 indicates that the 45° core of TH-26 exhibits somewhat high velocities (hence a high C_{13} constant) relative to the other cores. This may result in systematic errors between observed and calculated velocities for the *Vp* and *Vsv* velocity surfaces. To investigate this possibility, a least squares line was fit through the observed *Vp* measurements to estimate a 45° compressional wave velocity and hence a new C_{13} constant. In Figure 3, velocity surfaces calculated using the new, slightly lower C_{13} value are shown. Overall, the match between observed and calculated *Vp* and *Vsv* is improved, resulting in average differences of 1.0% and 2.4%, respectively.

Several interesting features can be seen on the phase velocity surfaces of Figures 1–3 which are worth further discussion. The calculated *Vsh* velocity surfaces indicate that a smooth increase in *Vsh* velocity should be seen in going from propagation perpendicular to bedding to propagation in the bedding plane. This is confirmed in a convincing manner for both TH-26 and TH-51 by the observed *Vsh* velocities. The *Vp* phase velocity surfaces also indicate that a smooth increase in compressional wave velocity should be seen in going from normal incidence to propagation in the bedding plane. Observed compressional wave velocities roughly confirm this trend, but exhibit scatter caused by compositional variation.

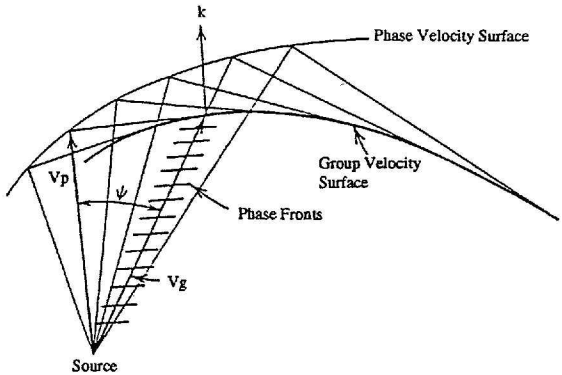

Fig. 4. Relationship between phase and group velocity surfaces showing phase velocity vector (Vp), group velocity vector (Vg), and angle between wavefront normal and group velocity direction (ψ). Modified from Auld (1990).

The most interesting features can be found on the *Vsv* phase velocity surfaces. Peaks in velocity are observed in the calculated curves for propagation at roughly 30–45° to the bedding normal. Measured *Vsv* velocities in the same interval are often 0.3–0.4 km/s faster than the velocities of the normal incidence shear wave (or the velocity of the *Vsv* wave propagating in the bedding plane), thus the calculated peaks are confirmed, although not perfectly, by the measured velocities. Interestingly, in the range 0–30° from bedding normal, observed *Vsv* velocities are equal to if not slightly greater than the observed *Vsh* velocities. This finding is predicted by the calculated velocity curves for both TH-26 and TH-51.

5. Phase or Group Velocity?

We have assumed that phase velocities are measured in non-symmetry directions for the calculation of the curves in Figures 1–3. For cores taken in symmetry axes directions, phase velocity is equivalent to group velocity (Musgrave, 1970). In non-symmetry directions, the raypath (group velocity) direction is, in general, not the same as the wavefront normal (phase velocity) direction (e.g., Auld, 1990; Cheadle *et al.*, 1991) (Figure 4). Group velocity implies point sources and receivers, and that we are measuring the traveltime of an "envelope" of plane waves as it travels through the sample core (Hearmon, 1961). Phase velocity implies planar sources and receivers which generate plane waves, and that we essentially measure the velocity of a wavefront advancing from source to receiver (Thomsen, 1986). The question of which velocity the pulse transmission technique obtains in non-symmetry directions has been the subject of controversy, with some believing that a group velocity is measured and others believing that the velocity measured is more closely approximated as a phase velocity (e.g., Crosson and Lin, 1971; Harder, 1985; Dellinger and Vernik, 1992; Vernik and Nur, 1992).

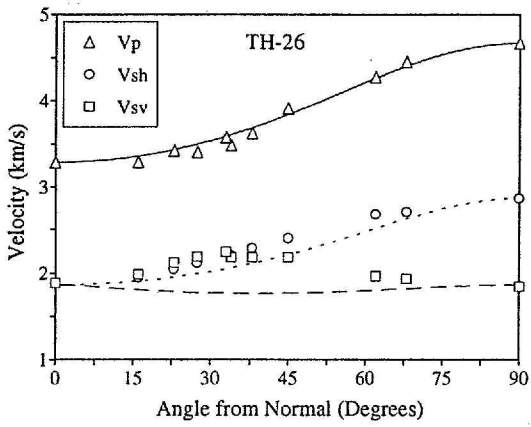

Fig. 5. Group velocity surfaces for TH-26 calculated assuming group velocities are measured in non-symmetry directions. Average differences between observed and calculated *Vp*, *Vsv*, and *Vsh* velocities are 1.4%, 15.0%, and 5.7%, respectively.

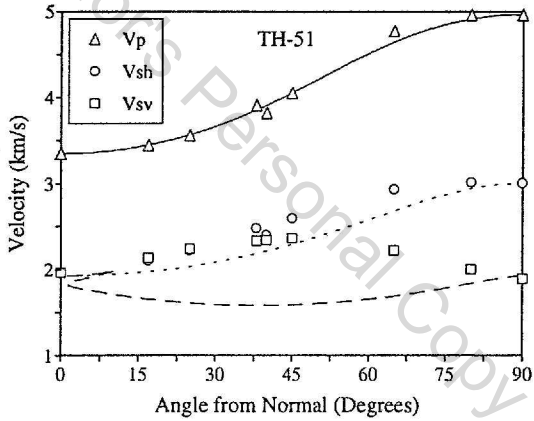

Fig. 6. Group velocity surfaces for TH-51 calculated assuming group velocities are measured in non-symmetry directions. Average differences between observed and calculated *Vp*, *Vsv*, and *Vsh* velocities are 1.1%, 25.6%, and 7.6%, respectively.

Cheadle *et al.* (1991) present equations for orthorhombic symmetry solids which can be easily modified (e.g., Eaton, 1993) to calculate the C_{13} constant of a transversely isotropic solid assuming *group* velocity is measured at 45°. Figures 5 and 6 show group velocity surfaces for TH-26 and TH-51 (Musgrave, 1970) calculated under this assumption. Again, measured velocities are shown which now show very poor agreement with the calculated values. Thus it appears that the velocities measured in non-symmetry directions using the pulse transmission technique are much more closely approximated as phase velocities, the same conclusion as that of Vernik and Nur (1992). Additional arguments for the phase velocity assumption include that the transducer diameters used in the

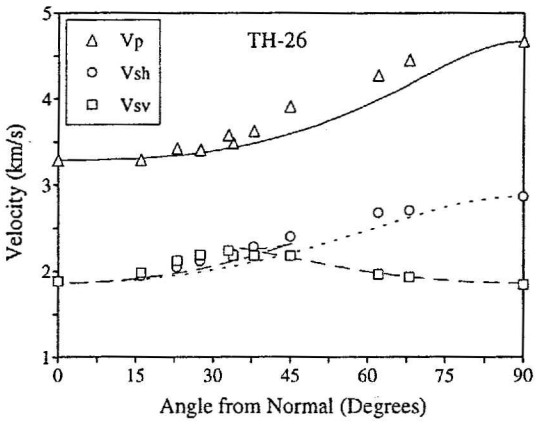

Fig. 7. Group velocity surfaces for TH-26. Measured phase velocities shown for reference. Note cusp on *Vsv* surface.

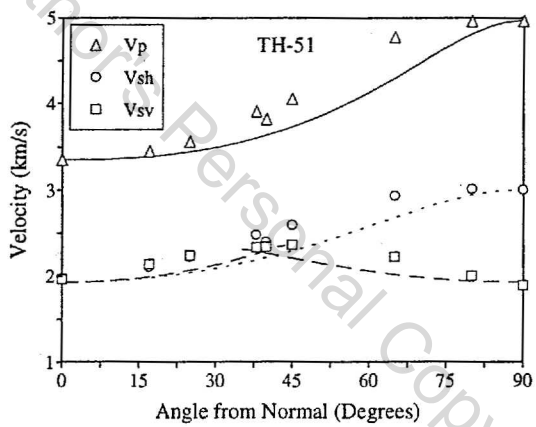

Fig. 8. Group velocity surfaces for TH-51. Measured phase velocities shown for reference.

measurements are the same as the sample diameters (2.54 cm), and the length of non-symmetry direction samples rarely exceeded 3.0 cm.

6. Group Velocity Surfaces

In Figures 7 and 8, "true" group velocity surfaces derived from the phase velocity surfaces of Figures 2 and 3 are shown for TH-26 and TH-51 at 100 MPa confining pressure. The equations in Hearmon (1961) and Musgrave (1970) were used to convert phase velocity vectors to corresponding group velocity vectors. Overall, a significant decrease in calculated velocities can be seen in non-symmetry directions, as group velocity is usually less than phase velocity for these propagation paths (Musgrave, 1970). The difference between phase and group velocity is significant for these shales due to their high anisotropy (Table II). The peaks

TABLE II
Calculated phase and group velocitie (in km/s) as a function of angle to bedding normal.

Angle	TH-26						TH-51					
	Vp		Vsv		Vsh		Vp		Vsv		Vsh	
(Degrees)	Phase	Group	Phase	Group	Phase	Group	Phase	Group	Phase	Group	Phase	Group
0	3.286	3.286	1.865	1.865	1.865	1.865	3.349	3.349	1.927	1.927	1.927	1.927
10	3.295	3.293	1.937	1.885	1.903	1.882	3.366	3.361	2.001	1.949	1.969	1.945
20	3.340	3.322	2.098	1.949	2.008	1.930	3.439	3.404	2.162	2.015	2.082	1.997
30	3.469	3.390	2.232	2.060	2.159	2.015	3.614	3.492	2.286	2.127	2.246	2.086
40	3.702	3.508	2.260	2.270	2.330	2.136	3.895	3.636	2.305	2.321	2.431	2.216
45	3.842	3.590	2.236	2.315	2.417	2.211	4.056	3.732	2.279	2.210	2.524	2.294
50	3.987	3.688	2.195	2.099	2.500	2.293	4.219	3.845	2.239	2.155	2.614	2.382
60	4.260	3.936	2.087	1.998	2.650	2.474	4.521	4.130	2.135	2.058	2.774	2.579
70	4.478	4.235	1.976	1.924	2.766	2.660	4.761	4.475	2.031	1.986	2.899	2.780
80	4.618	4.530	1.895	1.879	2.839	2.808	4.913	4.810	1.955	1.942	2.977	2.941
90	4.665	4.665	1.865	1.865	2.864	2.864	4.965	4.965	1.927	1.927	3.004	3.004

of the calculated *Vsv* phase velocity surfaces of TH-26 and TH-51 result in small "cusps" (obscured) in the corresponding *Vsv* group velocity curves. Very large cusps are possible for a given solid depending on the shape of the corresponding phase velocity surface (e.g., Musgrave, 1970).

7. Conclusions

This paper represents the preliminary results of an ongoing investigation of anisotropy and wave propagation in rocks. Future efforts will include examination of additional samples and more detailed analysis of wave propagation. Several important conclusions can be drawn from this study regarding highly anisotropic shales:

1) A comparison of the velocity data of Table I with previously published shale velocity data (Table III) emphasizes the highly anisotropic nature of the shales examined in this paper. TH-26 and TH-51 provide important examples of strong transverse isotropy caused by mineral alignment.
2) Multiple velocity measurements in non-symmetry directions provide important constraints on calculated elastic constants and velocity surfaces.
3) The velocities measured in non-symmetry directions appear to be more closely approximated as phase velocities.
4) *Vp* and *Vsh* phase velocities increase in going from normal incidence to propagation directions in the bedding plane, with the greatest rate of increase in the interval 20–70° from bedding normal.
5) Calculated and observed *Vsv* phase velocities achieve peak values approximately 30–45° from the bedding normal.
6) At near-normal incidence, approximately 0–30° from the bedding normal, *Vsv* is approximately equal to *Vsh*. Thus, conventional common depth point seismic data collected over highly anisotropic shales could be interpreted assuming *isotropic* lithologies due to the lack of shear wave splitting at near-normal incidence.
7) Due to the highly anisotropic nature of the shales, group velocities are significantly lower than phase velocities.

In typical field seismic investigations, subsurface lithologies are often assumed to be isotropic when in reality they are not. Depending on the relative anisotropy of the given formations, this assumption can lead to significant errors in estimating depths to reflectors (e.g., Banik, 1984; Thomsen, 1986). The effects of even mild anisotropy cannot be ignored in cross-borehole seismic tomography where the assumption of isotropy in a transversely isotropic formation can lead to significant imaging problems (Carrion *et al.*, 1992). The velocity surfaces presented here provide details of wave propagation in anisotropic shales and serve as a reminder of the extreme anisotropy possible in sedimentary sequences.

TABLE III

Summary of published laboratory anisotropy data for shales. Anisotropy is defined as $(V_{max} - V_{min})/V_{max}$ for a given rock sample.

Authors	Formation	Sample	Anisotropy (%) Vp	Anisotropy (%) Vs	Pressure (MPa)
This study	Chattanooga	TH-26	30	35	100
	"	TH-51	33	36	100
Jones and Wang (1981)	Pierre	3200 ft.	7	23	100
	Greenhorn	5000 ft.	16	24	100
Lo et al., (1986)	Chicopee Shale	shale	6	5	100
Vernik and Nur (1992)	Bakken	7570 ft.	21	18	70
	"	8634	27	30	"
	"	9831	18	10	"
	"	10,164	19	18	"
	"	10,487	24	23	"
	"	10,495	17	16	"
	"	10,575	25	19	"
	"	10,733	23	24	"
	"	10,734	21	26	"
	"	10,931	30	32	"
	"	10,932	22	23	"
	"	11,230	15	13	"
	"	11,246	15	13	"
	"	11,280	19	14	"

Acknowledgements

This paper benefited from the constructive comments of two anonymous reviewers. The assistance of D. Szymanski and N. Levine in sample collection is appreciated. Laboratory studies were supported by the Office of Naval Research contract N00014–89–J–1209.

References

Alexandrov, K.S. and Ryzhova, T.V.: 1961, 'Elastic Properties of Rock-Forming Minerals, 1, Pyroxenes and Amphiboles', *Bull. Acad. Sci. USSR, Geophys. Ser., English Trans.* **9**, 1165–1168.

Auld, B.A.: 1990, *Acoustic Fields and Waves in Solids, Vol. 1*, Robert E. Krieger Pub. Co., Malabar, Florida.

Babuska, V.: 1972, 'Elasticity and Anisotropy of Dunite and Bronzitite', *J. Geophys. Res.* **77**, 6955–6965.

Baker, D.W. and Carter, N.L.: 1972, 'Seismic Velocity Anisotropy Calculated for Ultramafic Minerals and Aggregates', *Am. Geophys. U. Mon.* **16**, 157–166.

Banik, N.C.: 1984, 'Velocity Anisotropy of Shales and Depth Estimation in the North Sea Basin', *Geophysics* **49**, 1411–1419.

Birch, F.: 1960, 'The Velocity of Compressional Waves in Rocks to 10 Kilobars, 1', *J. Geophys. Res.* **65**, 1083–1102.

Brocher, T. M. and Christensen, N.I.: 1990, 'Seismic Anisotropy Due to Preferred Mineral Orientation Observed in Shallow Crustal Rocks in Southern Alaska', *Geology* **18**, 737–740.

Carrion, P., Costa, J., Pinheiro, J.E.F. and Schoenberg, M.: 1992, 'Cross-Borehole Tomography in Anisotropic Media', *Geophysics* **57**, 1194–1198.

Cheadle, S.P., Brown, R.J. and Lawton, D.C.: 1991, 'Orthorhombic Anisotropy: A Physical Seismic Modeling Study', *Geophysics* **56**, 1603–1613.

Christensen, N.I.: 1966, 'Elasticity of Ultrabasic Rocks', *J. Geophys. Res.* **71**, 5921–5932.

Christensen, N. I. and Ramananantoandro, R.: 1971, 'Elastic Moduli and Anisotropy of Dunite to 10 Kilobars', *J. Geophys. Res.* **76**, 4003–4010.

Christensen, N.I.: 1984, 'The Magnitude, Symmetry, and Origin of Upper Mantle Anisotropy Based on Fabric Analyses of Ultramafic Tectonites', *Geophys. J. R. astr. Soc.* **76**, 89–111.

Christensen, N.I.: 1985, 'Measurements of Dynamic Properties of Rock at Elevated Temperatures and Pressures', in H.J. Pincus and E. R. Hoskins (eds.), *Measurements of Rock Properties at Elevated Temperatures and Pressures*, American Society for Testing and Materials, Philadelphia, Pa., pp 93–107.

Crampin, S.: 1985, 'Evaluation of Anisotropy by Shear Wave Splitting', *Geophysics* **50**, 142–152.

Crosson, R. L. and Lin, J.W.; 1971, 'Voigt and Reuss Prediction of Anisotropy Elasticity of Dunite', *J. Geophys. Res.* **76**, 570–578.

Dellinger, J. and Vernik, L.: 1992, 'Do Core Sample Measurements Record Phase or Group Velocity?', *62nd. Ann. Internat. Mtg., Soc. Explor. Geophys.* Expanded Abstracts, 662–665.

Eaton, D.W.: 1993, 'Discussion of "Ultrasonic Velocity and Anisotropy of Hydrocarbon Source Rocks" by Vernik, L. and Nur, A.', *Geophysics* **58**, 758–759.

Harder, S.: 1985, 'Inversion of Phase Velocities for the Anisotropic Elastic Tensor', *J. Geophys. Res.* **90**, 10,275–10,280.

Hearmon, R.F.S.: 1961, *An Introduction to Applied Anisotropic Elasticity*, Oxford University Press, Oxford.

Hess, H.H.; 1964, 'Seismic Anisotropy of the Uppermost Mantle Under Oceans', *Nature* **203**, 629–631.

Johnston, J.E. and Christensen, N.I.: 1992, 'Shear Wave Reflectivity, Anisotropies, Poisson's Ratios, and Densities of a Southern Appalachian Paleozoic Sedimentary Sequence', *Tectonophysics* **210**, 1–20.

Jones, L.E.A. and Wang, H.F.: 1981, 'Ultrasonic Velocities in Cretaceous Shales from the Williston Basin', *Geophysics* **46**, 288–297.

Justice, M.G., McCormack, M.D. and Lee, S.S.: 1986, 'Anisotropy in the Morrow Formation of Southeast New Mexico', in S.H. Danboom and S.N. Domenico (eds.), *Shear Wave Exploration*, Society of Exploration Geophysicists Geophysical Development Series, 1, pp. 154–164.

Kumazawa, M.: 1969, 'The Elastic Constants of Single Crystal Orthopyroxene', *J. Geophys. Res.* **74**, 5973–5980.

Lo, T., Coyner, K.B. and Toksoz, M.N.: 1986, 'Experimental Determination of Elastic Anisotropy of Berea Sandstone, Chicopee Shale, and Chelmsford Granite', *Geophysics* **51**, 164–171.

Lynn, H.B., and Thomsen L.A.: 1990, 'Reflection Shear Wave Data Collected Near the Principal Axes of Azimuthal Anisotropy', *Geophysics* **55**, 147–156.

McCormack, M.D., Dunbar, J.A. and Sharp, W.W.: 1984, 'A Case Study of Stratigraphic Interpretation Using Shear and Compressional Seismic Data', *Geophysics* **49**, 509–520.

Musgrave, M.J.P.: 1970, *Crystal Acoustics*, Holden Day, San Francisco.

Pacalo, R.E.G., Weidner, D.J. and Gasparik, T.: 1992, 'Elastic Properties of Sodium-Rich Majorite Garnet', *Geophys. Res. Lett.* **19**, 1895–1898.

Sano, O., Kudo, Y. and Mizuta, Y.: 1992, 'Experimental Determination of Elastic Constants of Oshima Granite, Barre Granite, and Chelmsford Granite', *J. Geophys. Res.* **97**, 3367–3379.

Seront, B., Mainprice, D. and Christensen, N. I.: 1993, 'A Determination of the Three Dimensional Seismic Properties of Anorthosite: Comparison Between Values Calculated from the Petrofabric and Direct Laboratory Measurements', *J. Geophys. Res.* **98**, 2209–2221.

Thomsen, L.: 1986, 'Weak Elastic Anisotropy', *Geophysics* **51**, 1954–1966.

Thomsen, L.: 1988, 'Reflection Seismology Over Azimuthially Anisotropic Media', *Geophysics* **53**, 304–313.

Verma, R. K.: 1960, 'Elasticity of Some High Density Crystals', *J. Geophys. Res.* **65**, 757–766.

Vernik, L. and Nur, A.: 1992, 'Ultrasonic Velocity and Anisotropy of Hydrocarbon Source Rocks', *Geophysics* **57**, 727–735.

Walker, K.R.: 1985, 'The Geologic History of the Thorn Hill Paleozoic Section (Cambrian-Mississippian) Eastern Tennessee', *Univ. Tennessee, Dept. Geol. Sci., Studies in Geology*, **10**, pp 1–128.

Weidner, D.J., Swyler, K. and Carleton, H.R.: 1975, 'Elasticity of Microcrystals', *Geophys. Res. Lett.* **2**, 189–192.

White, J.E., Martineau-Nicoletis, L. and Monash, C.: 1983, 'Measured Anisotropy in Pierre Shale', *Geophys. Prosp.* **31**, 709–725.

Winterstein, D.F.: 1986, 'Anisotropy Effects in P-wave and SH-wave Stacking Velocities Contain Information on Lithology', *Geophysics* **51**, 661–672.

Winterstein, D.F.: 1990, 'Velocity Anisotropy Terminology for Geophysicists', *Geophysics* **55**, 1070–1088.